Bioorganic & Medicinal Chemistry Letters 22 (2012) 4028–4032

Contents lists available at SciVerse ScienceDirect

Bioorganic & Medicinal Chemistry Letters

journal homepage: www.elsevier.com/locate/bmcl

Acylprolinamides: A new class of peptide deformylase inhibitors with in vivo antibacterial activity

Jeffrey M. Axten [a,*], Jesús R. Medina [a], Charles W. Blackledge [a], Céline Duquenne [a], Seth W. Grant [a], Mark A. Bobko [a], Tony Peng [a], William H. Miller [a], Theresa Pinckney [a], Timothy F. Gallagher [a], Swarupa Kulkarni [a], Thomas Lewandowski [a], Glenn S. Van Aller [a], Rimma Zonis [a], Paris Ward [b], Nino Campobasso [b]

[a] Infectious Diseases Center of Excellence for Drug Discovery, Antibacterial Discovery Performance Unit, GlaxoSmithKline, Collegeville, PA 19426, USA
[b] Computational and Structural Chemistry, GlaxoSmithKline, Collegeville, PA 19426, USA

ARTICLE INFO

Article history:
Received 6 March 2012
Revised 16 April 2012
Accepted 17 April 2012
Available online 25 April 2012

Keywords:
Peptide deformylase
PDF inhibitor
Antibacterial
Antibiotic

ABSTRACT

A new class of PDF inhibitor with potent, broad spectrum antibacterial activity is described. Optimization of blood stability and potency provided compounds with improved pharmacokinetics that were suitable for in vivo experiments. Compound **5c**, which has robust antibacterial activity, demonstrated efficacy in two respiratory tract infection models.

© 2012 Elsevier Ltd. All rights reserved.

The emergence of drug resistant bacteria continues to hamper the effectiveness of existing antibacterial agents. Demand for new classes of antibiotics to fight resistant bacteria stimulated a surge in research over the last 15 years to discover and develop antibiotics with new modes of action to treat infections resistant to common therapies. Drugs interfering with bacterial protein synthesis are proven and effective in treating hospital and community bacterial infections.[1] Therefore, unexploited protein synthesis machinery is attractive as a target for drug discovery and can offer advantages in avoiding resistance in the clinic. Peptide deformylase (PDF) is an essential bacterial metalloenzyme that catalyzes the hydrolytic removal of the *N*-formyl group from the terminal methionine during protein maturation.[2] Although bacterial PDF was identified more than 40 years ago,[3] it was not until the late 1990s that a stable preparation of the native enzyme was available, which led to assay development, screening and subsequent reports

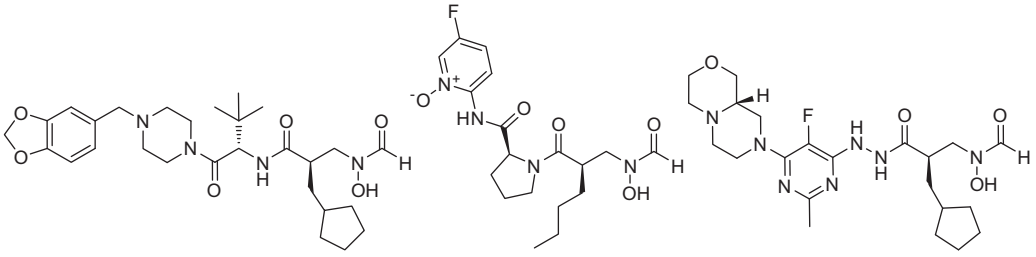

Figure 1. Structures of PDF inhibitors dosed in the clinic.

* Corresponding author. Tel.: +1 610 917 7899.
E-mail address: jeffrey.m.axten@gsk.com (J.M. Axten).

0960-894X/$ - see front matter © 2012 Elsevier Ltd. All rights reserved.
http://dx.doi.org/10.1016/j.bmcl.2012.04.086

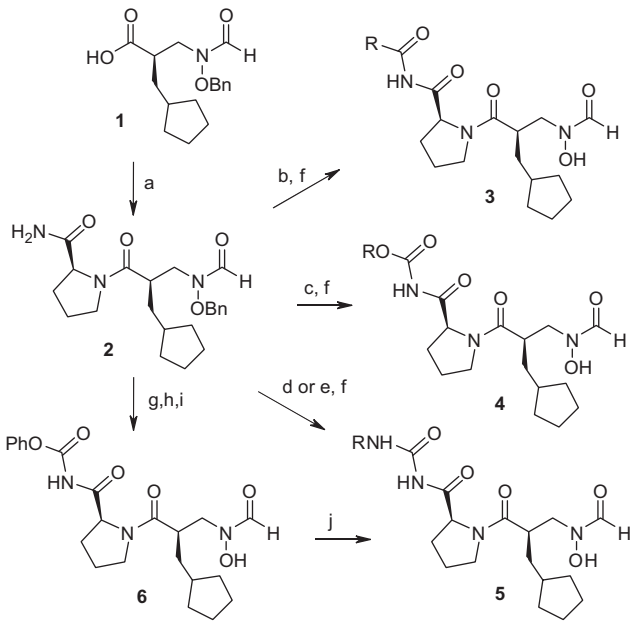

Scheme 1. (a) L-prolinamide, EDCI, HOBt, NMM, DMF; (b) R(C=O)Cl, LHMDS, THF, −78 °C; (c) RO(C=O)Cl, LHMDS, THF, −78 °C; (d) R1R2 N(C=O)Cl, LHMDS, THF, −78 °C; (e) RNCO, toluene, 120 °C; (f) H_2, Pd/BaSO4 (unreduced), MeOH; (g) H_2, Pd/C, MeOH; (h) TBDMSCl, imidazole, DMF; (i) PhO(C=O)Cl, LHMDS, THF, −78 °C, then 1 N HCl; (j) RNH_2, MeOH.

of a variety of inhibitor chemotypes and preclinical candidates.[4] The PDF inhibitors BB-83698,[5] LBM-415,[6] and GSK1322322[7] (Fig. 1) have advanced to clinical trials.

In the present Letter, we describe our discovery and evaluation of a series of PDF inhibitors based on an acylprolinamide template, as exemplified by structures **3–5** (Scheme 1).

The syntheses of compounds 3–5 is shown in Scheme 1.[8] The *N*-hydroxyformamide metal chelating functionality, and P1′ cyclopentyl methyl groups were selected based on historical SAR.[5–7] The key intermediate prolinamide **2** was prepared by standard coupling of the previously reported acid **1**[9] with L-prolinamide. The imides **3** and acylcarbamate derivatives **4** were prepared by acylation of the primary carboxamide with the corresponding acid chloride or chloroformate. The acylation can be carried out conveniently and efficiently by premixing the reactants in THF, and slowly adding 2–2.2 equiv of LHMDS at low temperature. Deprotection of the benzyl group afforded the *N*-hydroxyformamide **3** or **4**. The use of unreduced $Pd/BaSO_4$ is critical in most cases to minimize over-reduction to the formamide.[10] The acylurea analogs were prepared by several methods. Acylureas are accessible by substituting carbamoyl chlorides for acid chlorides as described above. When the isocyanate is available, heating with **2** neat or in toluene provides the acylureas. Subsequent deprotection of the benzyl group provided the *N*-hydroxyformamides **5**.

A higher throughput synthesis of acylureas, eliminating the use of isocyanates and the final hydrogenation step, was developed from compound **6** which can be easily prepared on large scale

Table 1
[a]PDF enzyme activity and antibacterial activity of acylprolinamides

Entry	R1	PDF IC_{50} (nM)			MIC (μg/mL)				
		S. a.	*S. p.*	*H. i.*	*S. a.*	*S. p.*	*H. i.*	*M. c.*	*E. f.*
					Oxford	1629	Q1	1502	7
3a	CH_3–	12	4	16	1	4	0.25	⩽0.06	8
3b	CH_3OCH_2–	8	1	13	4	4	0.125	⩽0.06	16
3c	$(CH_3)_2CH$–	5	1.5	10	2	2	0.5	⩽0.06	4
3d	$(CH_3)_2CHCH_2$–	4	0.8	7	1	1	0.5	⩽0.06	2
3e	$(CH_3)_3C$–	10	1.3	18	2	2	2	⩽0.06	4
3f	Cyclobutyl–	5	0.7	9	1	1	1	⩽0.06	8
3g	Cyclopropyl–	2.3	1.2	5.5	0.5	1	0.125	⩽0.06	2
3h	Cyclopentyl–	2.5	0.43	6.1	0.5	0.25	0.25	⩽0.06	1
3i	Cyclohexyl–	3.7	0.5	5.2	1	0.25	0.5	⩽0.06	1
3j	Phenyl–	5.2	0.28	3.8	1	0.25	0.5	⩽0.06	1
4a	CH_3–	4.5	1.9	13	1	1	0.125	⩽0.06	4
4b	CH_3CH_2–	2.2	0.54	7.7	0.5	0.5	0.25	⩽0.06	2
4c	$(CH_3)_2CH$–	2	0.48	4.7	0.25	0.25	0.25	⩽0.06	4
4d	$(CH_3)_3C$–	3.4	0.52	3.2	1	0.25	0.25	⩽0.06	1
4e	Cyclobutyl–	2.4	0.51	5.8	0.5	0.25	0.5	⩽0.06	1
4f	Cyclopentyl–	1.4	0.26	3.1	0.5	0.125	1	⩽0.06	1
4g	Cyclohexyl–	1.5	0.3	2.3	0.25	0.125	1	⩽0.06	0.5
4h	Pyran-4-yl–	4.4	0.66	3.1	1	0.25	0.5	⩽0.06	2
4i	Piperidine-4-yl–	5.9	1.4	2.7	>64	8	16	1	>64
5a	H	2.2	0.91	4.8	2	2	0.125	⩽0.06	4
5b	CH_3–	2.1	0.46	6.1	0.5	1	0.25	⩽0.06	4
5c	CH_3CH_2–	2	0.44	4.9	0.5	1	0.5	⩽0.06	2
5d	$(CH_3)_2CH$–	1.6	0.31	3	1	1	2	⩽0.06	4
5e	$(CH_3)_3C$–	1.2	0.22	2.4	1	0.125	1	⩽0.06	1
5f	Cyclobutyl	0.9	0.3	1.8	0.125	0.125	0.5	⩽0.06	1
5g	Cyclopentyl	0.52	0.1	2	0.5	0.125	2	⩽0.06	1
5h	Cyclohexyl	0.93	0.2	4	0.5	0.125	4	⩽0.06	2
5i	$PhCH_2$–	1.7	0.19	6.5	0.5	0.125	2	⩽0.06	0.5
5j	$Ph(CH_2)_2$–	0.86	0.12	3.6	⩽0.06	⩽0.06	4	⩽0.06	0.5
5k	$Ph(CH_2)_3$–	1	0.19	4.1	0.5	0.25	8	⩽0.06	2
5l	$H_2C{=}CHCH_2$–	10	2.1	20	0.5	1	1	⩽0.06	2
5m	4-pyridinyl-$(CH_2)_2$–	1.7	0.35	4.4	2	1	2	⩽0.06	8
5n	3-pyridinyl-$(CH_2)_2$–	1.4	0.37	4.7	2	1	2	⩽0.06	>64
5o	2-pyridinyl-$(CH_2)_2$–	1.4	0.35	5.9	1	0.5	1	⩽0.06	4
5p	2-pyraziny-$(CH_2)_2$–	1.4	0.41	6.1	2	1	2	⩽0.06	8

(*continued on next page*)

Table 1 (*continued*)

Entry	R1	PDF IC_{50} (nM)			MIC (μg/mL)				
		S. a.	*S. p.*	*H. i.*	*S. a.*	*S. p.*	*H. i.*	*M. c.*	*E. f.*
					Oxford	1629	Q1	1502	7
5q	$HO(CH_2)_2$–	3.8	1.1	8.8	4	2	0.5	0.125	32
5r	$HO(CH_2)_3$–	3.2	0.77	6.9	4	2	1	0.125	16
5s	$H_2N(CH_2)_2$–	2.3	0.38	7	16	16	>64	2	>64
5t	$H_2NC(O)(CH_2)_2$–	3.3	0.72	6.3	32	8	2	0.5	>64
5u	1H-imidazole-4-yl-$(CH_2)_2$–	1.3	0.15	4.3	64	8	16	0.5	>64

[b] *S. aureus*, *S. pneumoniae* or *H. influenzae* PDF activity was measured as previously described.[13] Enzyme activity was measured in a coupled assay system where formate released from substrate is oxidized by formate dehydrogenase thereby reducing one molecule of NAD–NADH resulting in an increase in absorbance at 340 nM. Enzyme reactions were initiated by adding PDF to 96 well plates containing all other assay components in a total volume of 50 μL. For *S. aureus* and *H. influenzae* PDF, final reaction conditions were 50 mM potassium phosphate (pH 7.6), 5 units/ml FDH, 7 mM NAD, 5% DMSO, 2 nM enzyme, and Km concentrations of fMAS peptide. Conditions for *S. pneumoniae* PDF were identical except that 2 mM NAD and 33 pM enzyme were used. Reaction velocities were measured for 20 min at 25 °C in a Molecular Devices SpectraMax plate reader. Data reported is the average of at least 2 runs.

[c] Whole-cell antimicrobial activity was determined by broth microdilution using the National Committee for Clinical Laboratory Standards (NCCLS) recommended procedure (Document M7-A4). The compound was tested in serial two-fold dilutions ranging from 0.06 to 64 mcg/ml. The minimum inhibitory concentration (MIC) was determined as the lowest concentration of compound that inhibited visible growth. A mirror reader was used to assist in determining the MIC endpoint.

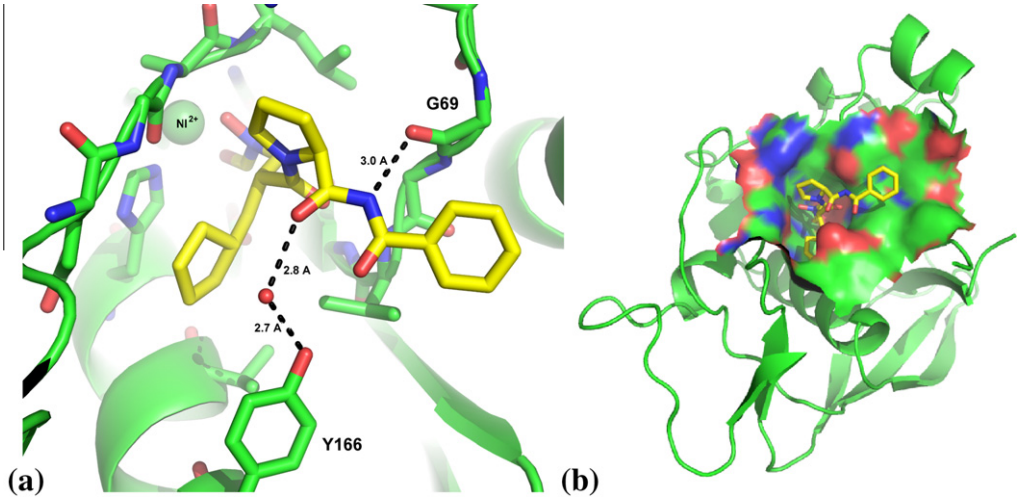

Figure 2. Crystal structure of **3j** (shown as yellow stick model) bound to *S. pneumoniae* PDF: (a) View of active site highlighting hydrogen bonding of the acylprolinamide; (b) view showing surface channel occupied by phenyl group of the imide.

without the need for chromatography (Scheme 1). The prolinamide **2** was converted to the TBDMS protected *N*-hydroxyformamide, and acylated with phenyl chloroformate to provide **6** after acidic aqueous workup. Since the acylureas can be easily prepared from **6** by mixing with an amine in suitable solvent, this was our preferred synthetic route for acylurea analog preparation.

The imides prepared were found to be very potent PDF inhibitors. Table 1 illustrates a range of substitution that is tolerated. The acetyl imide **3a** has the weakest potency, with IC_{50}s for the *Staphylococcus aureus* and *Streptococcus pneumoniae* PDF enzymes of 12 and 4 nM, respectively. As the alkyl group of the acyl imide is extended and branched the activity slightly improves, however the *tert*-butyl analog **3e** exhibits a slight loss in activity with a corresponding increase in MIC. The cycloalkyl and phenyl analogs **3f–j** generally are more potent enzyme inhibitors, and have favorable antibacterial activity against *S. aureus* and *S. pneumoniae*.

An X-ray crystal structure of **3j** bound to *S. pneumoniae* PDF was solved at 1.8 Å resolution (Fig. 2).[11] As shown in Figure 2a, the *N*-hydroxyformamide is bound to the active site metal (Ni^{2+}) and the cyclopentylmethyl group fills the P1′ pocket. The proline imide carbonyl interacts with the protein through hydrogen bonding to a conserved water and the OH of Y166, and the imide NH is engaged in hydrogen bonding with the carbonyl of a backbone glycine. The phenyl moiety occupies a large surface channel (Fig. 2b) that can accept a wide range of functionality of various sizes (see Table 1). Consequently, we directed our research to the optimization of the physical properties and pharmacokinetics by modifying the group that projects into this channel.

Imides **3a–j** generally have poor oral availability and very high clearance in rats, consistent with our finding that they are not

Table 2
[a] Blood stability data for acylprolinamide derivatives in rat and human blood

Entry	% recovery @ 2 h	
	Rat	Human
3e	29.0 ± 21.0	80.6 ± 7.3
3j	27.2 ± 10.5	NT
4c	0	49.6 ± 14.4
4d	27.6 ± 31.6	52.0 ± 10.4
4e	0	31.7 ± 15.3
4f	0	57.5 ± 10.0
4g	0.4 ± 39.1	45.8 ± 6.4
4h	9.5 ± 18.6	23 ± 16.9
5c	58.6 ± 19.4	110.9 ± 15.3
5d	NT	99.7 ± 1.5
5g	NT	103 ± 11.3
5j	NT	92.2 ± 9.4

[a] Samples ($n = 3$) were spiked into fresh human blood to yield target concentrations of 2000 ng/mL and incubated at 37 °C for 120 min. NT = not tested.

Table 3
Pharmacokinetic data ($n = 3$) for compound **5c**

	i.v.		p.o.		
	Dose (mg/kg)	Cl_p (ml/min/kg)	Dose (mg/kg)	DNAUC[a]$_{(0-inf)}$ (ng.h/mL/mg/kg)	%F
Rat	2.5	119.9 ± 14.8	27.1	43.3 ± 0.6	~30[b]
Dog	4.5	36.3 ± 4.1	6.5	629.9 ± 46.9	100 ± ND
Monkey	3.0	29.4 ± 3.3	5.1	111.4 ± 42.1	20 ± 9

[a] Cl_p = plasma clearance; DNAUC = dose normalized AUC; F = oral bioavailability.
[b] Estimated from a non-crossover study.

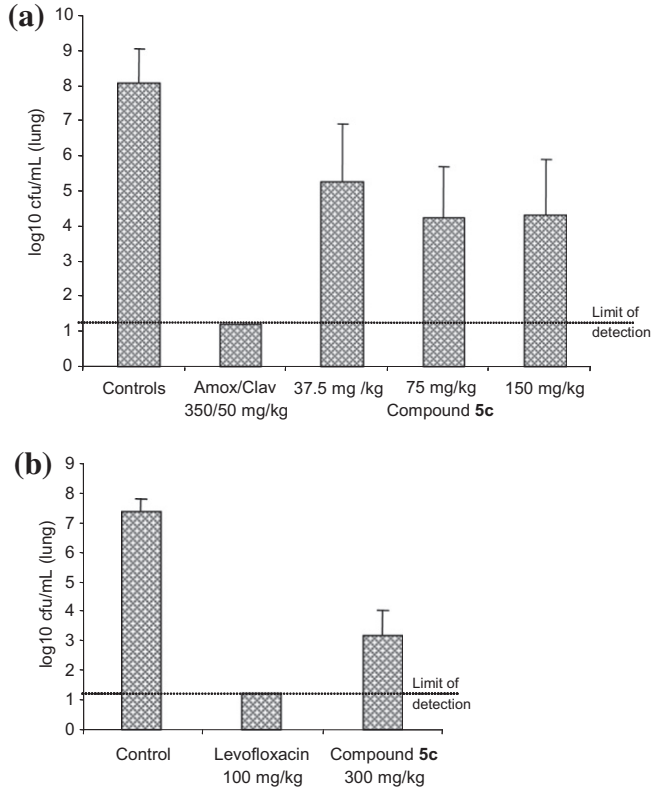

Figure 3. $N = 6$ for each group. (a) Efficacy of compound **5c** (MIC = 0.25 μg/mL) and amoxicillin/clavulinic acid (MIC = 0.03 μg/mL) in a *S. pneumoniae* 1629 rat respiratory tract infection model. Compounds were dosed orally b.i.d. for 4 days starting 1 h post-infection; (b) efficay of compound **5c** (MIC = 1 μg/mL) and Levofloxacin (MIC = 0.016 μg/mL) in an *H. influenzae* H-128 rat respiratory tract infection model. Compounds were dosed orally b.i.d. for 2 days starting 1 h post-infection.

stable in blood (Table 2). We suspected that the susceptibility of imides to degradation by esterases and amidases was the primary source of this instability. We reasoned that the blood stability might be improved if the imide carbonyl was less electrophilic. This led to the synthesis of the acylcarbamates **4** and acylureas **5**. Although there was little improvement in stability of the acylcarbamates **4**, there was a dramatic improvement in blood stability of the acylureas **5**, particularly in human blood, where >89% of compounds remained after a 2 h incubation.

The acylcarbamates and acylureas maintained good antibacterial potency and spectrum. The acylcarbamates **4a–i** have slightly increased potency in the enzyme assay, but display remarkable improvement in antibacterial activity, particularly against *S. pneumoniae* 1629 (see Table 1). The acylcarbamates **4a–h** and acylureas **5a–p** also display very potent enzyme inhibition, generally <10 nM, coupled with potent antibacterial activity against *S. aureus, S. pneumoniae*, *Haemophilus influenzae* and *Moraxella catarrhalis*. Although target potency is similar amongst the compounds, the antibacterial activity varies and is likely related to changes in lipophilicity, with more polar analogs exhibiting much higher MICs. For example, primary alcohols (**5q** and **5r**) have slightly diminished antibacterial activity, whereas the more polar amine and imidazole derived analogs (**4i**, **5s–u**) are significantly less active in the whole cell assay even though they maintain potent enzyme activity. This might be due to decreased permeability or increased bacterial efflux.

Compound **5c** was selected for in vivo studies based on its blood stability and robust activity in broader antibacterial profiling. Pharmacokinetic data is shown in Table 3.[12] In rats, Compound **5c** has high clearance and 30% bioavailability. The high clearance impacts the exposure indicated by the relatively low DNAUC. In dogs and monkeys, compound **5c** has good exposure and exhibits moderate to high clearance at low doses, with 100% and 20% bioavailability, respectively.

The efficacy of acylurea **5c** was evaluated in rat respiratory tract infection models.[12] Oral b.i.d. dosing (4 days) resulted in a reduction of *S. pneumoniae* 1629 bacterial lung counts, with decreases as high as 3.86 $\log_{10}$ cfu/mL at the 75 and 150 mg/kg doses compared to the non-treated control (Fig. 3a). Additionally, compound **5c** was effective against *H. influenzae* H-128 when dosed b.i.d. for 2 days at a dose of 300 mg/kg, reducing bacterial counts by 4.21 $\log_{10}$ cfu/mL (Fig. 3b).

In summary, we have discovered a new class of PDF inhibitors containing an acylprolinamide functionality. Lead compounds from this class have potent, broad spectrum antibacterial activity against major pathogens prevalent in community acquired bacterial infections. Adjusting the electrophilicity to enhance the blood stability of the acylprolinamide functionality led to acylureas, which have desirable physiochemical properties and pharmacokinetics. In vivo efficacy was demonstrated with compound **5c** in rat lung infection models of *S. pneumoniae* and *H. influenzae*, highlighting the utility of the acylprolinamide class of PDF inhibitors as antibacterial agents.

References and notes

1. a Wilson, D. N.; Stelzl, U.; Nierhaus, Knud H. In *Handbook of Proteins*; Cox, M. M.; Phillips, G. N., Eds.; 2007; Vol. 1, pp 258.; (b) Coyle, E. A. *Pharmacotherapy* **2003**, *23*, 638.
2. (a) Giglione, C.; Pierre, M.; Meinnel, T. *Mol. Microbiol.* **2000**, *36*, 1197; (b) Leeds, J. A.; Dean, C. R. *Curr. Opin. Pharmacol.* **2006**, *6*, 445; (c) Johnson, K. W.; Lofland, D.; Moser, H. E. *Curr. Drug Targets Infect. Disord.* **2005**, *5*, 39.
3. Adams, J. M. *J. Mol. Biol.* **1968**, *33*, 571.
4. For a historical account see: Yuan, Z. Y.; White, R. J. *Biochem. Pharmacol.* **2006**, *71*, 1042.
5. Ramanathan-Girish, S.; McColm, J.; Clements, J. M.; Taupin, P.; Barrowcliff, S.; Hevizi, J.; Safrin, S.; Moore, C.; Patuo, G.; Moser, H.; Gadd, A.; Hoch, U.; Jiang, V.; Loftland, D.; Johnson, K. W. *Antimicrob. Agents Chemother.* **2004**, *48*, 4835.
6. (a) McIntyre, J. A.; Castañer, J.; Martín *Drugs Future* **2005**, *30*, 23; (b) Sun, H.; MacLeod, C.; Zheng, W.; Dobson, C.; Skerjanec, A. *33rd Ann. Meet. Amer. Coll. Clin. Pharmacol.*, (Oct 3–5, Phoenix), **2004**, Abstract 30.
7. Qin, D.; Fang, Y.; Benowitz, A.; Liao, X.; Karpinski, J.; Dreabit, J.; Knox, A.; Kelly, S.; Axten, J.; Mercer, D.; Kulkarni, S.; Campobasso, N.; Zonis, R.; VanAller, G.; Christensen, S.; Zalacain, M.; Aubart, K. *50th Ann. ICAAC Meet.*, September 2010, Boston, MA, Abstract F1–2111.
8. Axten, J. M.; Medina, J. R. International Patent Appln. No. WO 2007016364 A2, International Publication Date: February 8, 2007.

9. Qin, D.; Norton, B.; Liao, X.; Knox, A.N.; Fang, Y.; Lee, J.; Dreabit, J.C.; Christensen, S.B.; Benowitz, A.B.; Aubart, K.M. *PCT Int. Appl.* 2009, WO2009061879A1.
10. Nikam, S. S.; Komberg, B. E.; Johnson, D. R.; Doherty, A. M. *Tetrahedron Lett.* **1995**, *36*, 197.
11. At 15.5 mg/ml, *Streptococcus pneumoniae* PDF was complexed with 1 mM **3j** for 16 h at 4 °C, drops were applied using the mosquito and grown over a period of 2–8 days at 22 °C in a 400 nL hanging drop. The drop was composed of 200 nL of the protein/inhibitor complex, 50 nL of previously grown crushed crystals (seeds suspended in ~3.3 M AmSO4, 3% Peg 400 and 0.1 M Hepes pH 7.5) from apo *Streptococcus pneumoniae* PDF and 150 nL well composition 0.2 M Potassium fluoride and 20% (w/v) PEG 3350. X-ray diffraction data were collected at the Advanced Photon Source on sector 21f, the Life Sciences Collaborative Access Team. The structure was solved by molecular replacement and refined with Phenix. Refine (Adams, P. D.; Grosse-Kunstleve, R. W.; Hung, L.-W.; Ioerger, T. R.; McCoy, A. J.; Moriarty, N. W.; Read, R. J.; Sacchettini, J. C.; Sauter, N. K.; Terwilliger, T. C.. *Acta Crystallogr., Sect. D: Biol. Crystallogr*. **2002**, *58*, 1948–1954). The model was built with COOT ('Coot: model-building tools for molecular graphics' Emsley, P.; Cowtan, K. *Acta Crystallogr., Sect. D: Biol. Crystallogr.* **2004**, *60*, 2126–2132 Part 12). Figures were made with Pymol (DeLano, Warren L. The PyMOL Molecular Graphics System, **2009**. DeLano Scientific LLC, Palo Alto, California, USA. http://www.pymol.org). X-ray data were submitted to the Protein Data Bank (PDB ID = 4EOX).
12. All studies were conducted after review by the GSK Institutional Animal Care and Use Committee and in accordance with the GSK Policy on the Care, Welfare and Treatment of Laboratory Animals.
13. (a) Lazennec, C.; Meinnel, T. *Anal. Biochem.* **1997**, *244*, 180; (b) Van Aller, G. S.; Nandigama, R.; Petit, C. M.; DeWolf, W. E.; Quinn, C. J.; Aubart, K. M.; Zalacain, M.; Christensen, S. B.; Copeland, R. A.; Lai, Z. *Biochem.* **2005**, *44*, 253.